Biophysical Chemistry 7 (1978) 235–252.


# MOLECULAR WEIGHT OF T2 NaDNA FROM VISCOELASTICITY

Brian C. BOWEN and Bruno H. ZIMM
*Department of Chemistry, B-017, University of California, San Diego, La Jolla, California, 92093, U.S.A.*

Received 13 May 1977

The viscoelastic properties of T2 DNA solutions are used to determine the NaDNA molecular weight in four independent ways from the theory of the beads-springs model. The four molecular weights are 131.9, 132.7, 130.5, and 127.6 × $10^6$. The average of these values, adjusted for the probable errors in viscoelasticity and concentration measurements, is (126 ± 5) × $10^6$. The four molecular weights are termed $M_{\tau\Gamma 11}$, $M_{\tau\eta}$, $M_{\tau\Gamma}$, and $M_{\tau A}$; each is different in its sensitivity to molecular weight distribution. Their agreement suggests (1) that the theoretical equations relating each $M$ to the corresponding measured properties are valid, (2) that T2 DNA behaves as a partially free-draining polymer chain, and (3) that our solutions were nearly homogeneous in DNA size. We show that serious errors can result if the viscoelastic properties are not extrapolated to their limits at zero shear rate, as well as at zero DNA concentration, before calculating molecular weight.

## 1. Introduction

Large DNA molecules exhibit the phenomenon of viscoelasticity. This is observed in a creep-recovery type of experiment in which the molecules are extended by an externally-applied, shearing stress and then allowed to relax in the absence of that stress [1-3]. While the molecules are extended in steady-state shearing, the viscosity of a DNA solution can be measured. During relaxation, at least four additional properties are measurable: $\Gamma$, the total amplitude of the elastic recoil; $A$, the time integral under the recoil curve; $\tau_{11}$ and $\Gamma_{11}$, the retardation time and recoil amplitude due to the largest molecular species in its longest relaxation mode.

As demonstrated here for T2 DNA, combinations of the five properties can be used to calculate four independent, "characteristic" molecular weights. Previous viscoelasticity measurements have been performed on DNA solutions from T2 bacteriophage [4], E. coli and B. subtilis [5], Drosophila [6], aberrant T2 phage [7], E. coli [8], yeast [9], and blue-green algae [10]. For the most part, only two of the viscoelastic properties, the specific viscosity ($\eta_{sp}$) and $\tau_{11}$, were used to calculate molecular weights in these papers, although some use of the other properties was made by Kavenoff and Zimm [6] and Uhlenhopp, Zimm and Cummings [7].

The four molecular weights are $M_{\tau\Gamma 11}$, $M_{\tau\eta}$, $M_{\tau\Gamma}$, and $M_{\tau A}$, where the subscripts refer to the characteristic set of properties from which each $M$ is calculated. The results for T2 DNA are 131.9, 132.7, 130.5, and 127.6 × $10^6$, respectively; they do not depend upon constants which must be obtained from empirical curves. They differ, however, from the usual viscosity-average and sedimentation-average molecular weights in that they are not averages (see remarks at end of Theory section (a)).

The good agreement between the characteristic $M$'s implies that the theory of DNA viscoelasticity from which they are derived is internally consistent and that the solutions contained primarily intact T2 DNA molecules. The mean of the characteristic $M$'s was (130.7 ± 1.6) × $10^6$, but this value does not include an error estimate for measurement of DNA concentration (each $M$ is proportional to concentration). When this estimate is included, the mean molecular weight becomes (126 ± 5) × $10^6$. This value may be compared with previous values determined by other techniques [11–15]. These are summarized in table 5; they range from 105.7 to 132 × $10^6$. A previous result obtained by viscoelastic measurements is 115 × $10^6$ [4].

In addition to the determination of molecular weight, this paper is concerned with the dependence of viscoelastic properties on shear rate. This dependence, except for the property $\eta_{sp}$, has been neglected in previous viscoelasticity measurements cited above, probably because of limited data accuracy. With improved instrumentation, it has become possible to demonstrate the dependence, and to show that it is necessary to extrapolate measured properties to zero shear rate, as well as to zero DNA concentration.

## 2. Materials and methods

### 2.1. Preparation of phage T2

E. coli B were grown at 37°C in three liters of M9 salts medium [16] supplemented with 1% Casamino acids and 0.4% glucose. At a concentration of about $5 \times 10^7$ cells/ml the culture was infected with $5 \times 10^5$ T2 phage/ml. Incubation was continued for 5.5 h, at which time the glucose concentration was increased by 0.25%. After seven hours, chloroform was added to enhance bacterial lysis. All subsequent manipulations were done at 4°C. The phage were purified by two cycles of low, high, and low-speed centrifugation. After each high-speed centrifugation, the phage pellet was covered with about twice its volume of 0.005 M $MgCl_2$, 0.01 M Tris buffer (pH 7.5). The covered pellets were left at 4°C for a few hours and then resuspended by gentle shaking. The titre of this purified phage stock was $4.5 \times 10^{12}$ PFU/ml.

### 2.2. Purification of DNA

An aliquot of the T2 phage stock was subjected to a low-speed centrifugation (5000 rpm or 10 min) in the Sorvall SS34 rotor. The supernatant was diluted four-fold with 1M-BPES buffer and then extracted by the hot phenol method of Massie and Zimm [17]. After four extractions the aqueous, DNA-containing phase was clear at room temperature. Three additional extractions gave the same experimental results (see below). Phenol was removed (determined spectrophotometrically) from the aqueous phase by dialysis against 1M BPES and then BBES buffer [18]. The purified T2 DNA was stored in BBES or BBESD (0.01 M $Na_2B_4O_7$, 0.001 M $Na_2EDTA$, 0.007 M Na dodecyl sulfate, 0.171 M NaCl, pH 8.9) in screw-cap polystyrene test tubes.

### 2.3. Preparation of solutions

DNA concentrations in stock solutions were measured spectrophotometrically assuming that 55.2 μg/ml DNA gives an absorbance of unity [19]. Quantitative dilutions were made by careful pouring and weighing. The method of dilution was:

(i) Stock T2 DNA solutions (about 100–125 μg/ml) were diluted with glycerol (Mallinckrodt, Analytical Reagent) in the proportion, 3 g glycerol to 1 g stock solution.

(ii) The tubes were placed in a horizontal position on a mechanical rotator, and mixed by rotation (at 8 rpm) until Schlieren patterns disappeared (about two hours).

(iii) Solutions were then stored overnight at 4°C.

(iv) The mixing procedure was repeated for 30 to 60 min before making further dilutions with the solvent, 75% glycerol – 25% BBES (weight per cent) or 75% glycerol – 25% BBESD.

(v) Subsequent dilutions were followed by 30 to 60 min of mixing, storage at 4° for at least six hours, 15 to 30 min of mixing, and then viscoelastic measurements.

The storage steps in the above procedure appeared to be necessary for dispersal of DNA molecules after dilution from a higher concentration (B. Bowen and R. Kavenoff, unpublished observations; J. Harpst, personal communication). For the glycerol-buffer solvent, $\rho_{23.5°C} = 1.19$ g/ml (determined pycnometrically). For the stock solutions of DNA in BBES or BBESD, $\rho_{23.5°C} = 1.00$ g/ml. DNA concentrations in glycerol-buffer solutions were calculated using these densities and were verified by absorbance in one set of experiments. Final sodium ion concentration was 0.06 M.

### 2.4. Viscoelastic measurements

The determination of viscoelastic solution properties using a Couette-type viscometer has been described previously [5–7,20]. Basically, one measures the angular position $\theta(t)$ of a rotating inner cylinder (rotor) which is suspended in the DNA solution. The rotor can be turned by the interaction of a metal ring

in the cylinder with a rotating magnetic field. When the the field is removed ($t = 0$), the rotor recoils in response to the relaxation of the elongated DNA molecules. As these molecules relax to their equilibrium, random-coil configurations, the rotor angle decays approximately exponentially from $\theta(0)$ to a baseline value $\theta(\infty)$.

If the rotor is turned for a long time relative to the longest relaxation time of the DMA molecules, the latter reach a steady-state extension, and the rotor angular velocity becomes constant. This is called a steady-state wind-up. The viscoelastic parameters obtained during one experimental run are

(i) $\omega = 360/T$ (deg/s), the rotor angular velocity during the wind-up, where $T$ is the time per revolution;

(ii) $\Gamma = \theta(0) - \theta(\infty)$ (deg), the total amplitude of the rotor recoil;

(iii) $A = \int_0^\infty [\theta(t) - \theta(\infty)]\,dt$ (deg-s), the time integral of the recoil;

(iv) $\tau_{11}$ (s), the retardation time associated with the longest (or principal) relaxation mode of the largest molecules in the solution;

(v) $\Gamma_{11}$ (deg), the amplitude of the rotor recoil due to the largest molecules in their longest (or principal) relaxation mode.

The quantities $\tau_{11}$ and $\Gamma_{11}$ are found by plotting $\ln[\theta(t) - \theta(\infty)]$ versus time. The curve exhibits a long-time linear portion with intercept equal to $\ln \Gamma_{11}$ and slope equal to the negative reciprocal of $\tau_{11}$. The specific viscosity $\eta_{sp}$, or the relative viscosity $\eta_{rel}$, may be calculated from $\omega$ once the rotor angular velocity in pure solvent, $\omega_s$, is known,

$$\eta_{sp} = \eta_{rel} - 1 = \omega_s/\omega - 1 = T/T_s - 1 . \tag{1}$$

The average shear rate $\kappa$ during a steady-state wind-up can be calculated from the equation of Zimm and Crothers [21],

$$\frac{S}{\eta} = \kappa = \pi\Omega \frac{R_1 + R_2}{R_2 - R_1} f(R_1, R_2) , \tag{2}$$

where $S$ = average shear stress (dyne/cm$^2$), $\eta$ = solution viscosity (poise), $\Omega = \omega/360$ (rev/s), $R_1$ = rotor radius (cm), $R_2$ = stator radius (cm), and $f(R_1, R_2)$ is a correction factor for concentric-cylinder viscometers. Also, if one measures $\Omega$ for a solvent of known viscosity, then $S$ corresponding to a given magnetic field strength can be determined. We calculated shear stresses from rotor velocities in a 30% sucrose solution at 25°C ($\eta = 0.02739$ poise, [22]). For the instrument used in these experiments $R_1 = 0.25$ cm and $R_2 = 0.40$ cm, so that

$$\kappa = 12.426\,\Omega = \left(\frac{12.426}{360}\right)\omega . \tag{3}$$

The factor (12.426/360) was used to convert measurements from degrees of rotor rotation to radians of shear. Details of the design and construction of the apparatus are given elsewhere [23]. All viscoelastic measurements were made at $T = 25$°C.

## 3. Theory

### 3.1. Characteristic molecular weights

When $\eta_{sp}$, $\tau_{11}$, $\Gamma_{11}$, $\Gamma$, and $A$ for a DNA solution at infinite dilution and under vanishingly small stresses are known, it is possible to calculate four independent molecular weights. These are called characteristic molecular weights because each is defined by a characteristic set of viscoelastic properties of the solution.

The beads-springs theory (24,25) of macromolecular behavior in infinitely dilute solutions predicts that for molecule $i$ [‡],

$$\tau_{i1} = \left(\frac{\eta_s}{S_1 RT}\right)[\eta_{sp}/C]_i M_i = K_\tau [\eta_{sp}/C]_i M_i , \tag{4}$$

where $\tau_{i1}$ is the relaxation time in the first normal mode, $\eta_s$ is the solvent viscosity, $[\eta_{sp}/C]_i$ is the limiting viscosity number, $M_i$ is the molecular weight, and $S_1$ is a theoretical constant (see below). In general, $[\eta_{sp}/C]_i$ may be related to $M_i$ alone using an empirical equation,

$$[\eta_{sp}/C]_i = K_\eta M_i^a , \tag{5}$$

where $K_\eta$ and $a$ are constants. Eqs. (4) and (5) may be combined to give

$$\tau_{i1} = K_\tau K_\eta M_i^{1+a} . \tag{6}$$

‡Throughout this paper, we will represent the limiting viscosity number, or intrinsic viscosity, by $[\eta_{sp}/C]$ rather than by $[\eta]$. This nomenclature is consistent with other limiting quantities which we calculate.

Consider a heterogeneous solution containing concentrations $C_i$, or number density $L_i$, of DNA molecules of molecular weight $M_i$, where $i = 1, 2, ..., P$. Following the method of Klotz and Zimm [20], we let

$$C = \sum_{i=1}^{P} C_i , \tag{7}$$

be the total concentration of DNA molecules, and

$$L = \sum_{i=1}^{P} L_i = \sum_{i=1}^{P} N_a\left(\frac{C_i}{M_i}\right), \tag{8}$$

be the total number of DNA molecules per unit volume. Then, the limiting viscosity number of the solution is related to each $M_i$ by

$$[\eta_{sp}/C] = \frac{\Sigma_{i=1}^{P} C_i [\eta_{sp}/C]_i}{\Sigma_{i=1}^{P} C_i} = K_\eta \frac{\Sigma_{i=1}^{P} C_i M_i^a}{\Sigma_{i=1}^{P} C_i} . \tag{9}$$

In the following equations, we will omit the brackets around $\eta_{sp}/C$ because we assume the solution of DNA molecules to be infinitely dilute. The average longest relaxation time $\langle \tau_1 \rangle$ for the solution is related to each $M_i$ by

$$\langle \tau_1 \rangle = \sum_{i=1}^{P} \frac{L_i}{L} \tau_{i1} = \frac{K_\tau K_\eta}{\Sigma_{j=1}^{P} (C_j/M_j)} \sum_i C_i M_i^a . \tag{10}$$

Similarly,

$$\langle \tau_1^2 \rangle = \frac{(K_\tau K_\eta)^2}{\Sigma_{j=1}^{P} (C_j/M_j)} \sum_{i=1}^{P} C_i M_i^{1+2a} . \tag{11}$$

$$\langle \tau_1^3 \rangle = \frac{(K_\tau K_\eta)^3}{\Sigma_{j=1}^{P} (C_j/M_j)} \sum_{i=1}^{P} C_i M_i^{2+3a} , \tag{12}$$

Eqs. (9), (10), (11), and (12) enable us to derive various molecular weight formulas for heterogeneous DNA solutions.

We start with an equation similar to eq. (4) to define the characteristic molecular weight, $M_{\tau\eta}$,

$$M_{\tau\eta} = \frac{S_1 RT}{\eta_s} \frac{\tau_{11}}{\eta_{sp/C}} , \tag{13}$$

From eqs. (6) and (9) we may write

$$\frac{\tau_{11}}{\eta_{sp}/C} = K_\tau \frac{M_1 \Sigma_{i=1}^{P} C_i}{\Sigma_{i=1}^{P} C_i (M_i/M_1)^a} ,$$

so that

$$M_{\tau\eta} = M_1 \frac{\Sigma_{i=1}^{P} C_i}{\Sigma_{i=1}^{P} C_i (M_i/M_1)^a} . \tag{14}$$

A second characteristic molecular weight $M_{\tau\Gamma 11}$ is derived from an expression for the magnitude of $\Gamma_{11}$ (see eq. (18) in ref. [20]),

$$\Gamma_{11} = \frac{\omega \eta_{sp} \nu}{S_1 \eta_{rel}} \frac{f_1 \tau_{11}^2}{\langle \tau_1 \rangle} , \tag{15}$$

where $f_1 = L_1/L$ and $\nu = 1$ (linear molecules) or 2 (circular molecules). Rearranging and substituting from eqs. (8), (9), and (10) gives

$$\frac{RT\nu\omega\tau_{11}^2 C}{\eta_s \eta_{rel} \Gamma_{11}} = M_1 \frac{\Sigma_{i=1}^{P} C_i}{C_1} . \tag{16}$$

The right-hand side of eq. (16) is a molecular weight which we can define as

$$M_{\tau\Gamma 11} = \frac{RT\nu\omega\tau_{11}^2 C}{\eta_s \eta_{rel} \Gamma_{11}} = M_1 \frac{\Sigma_{i=1}^{P} C_i}{C_1} . \tag{17}$$

A third value, $M_{\tau\Gamma}$, is obtained from eq. (17) of Klotz and Zimm [20] for the amplitude of the total recoil,

$$\Gamma = \frac{\omega \eta_{sp}}{\eta_{rel}} \frac{S_2}{S_1} \frac{\langle \tau_1^2 \rangle}{\langle \tau_1 \rangle} , \tag{18}$$

where $S_2$ is a constant (see below). Division by eq. (15) gives

$$\frac{\Gamma_{11}}{\Gamma} = \frac{\nu}{S_2} \frac{f_1 \tau_{11}^2}{\langle \tau_1^2 \rangle} . \tag{19}$$

Combining eqs. (19) and (16) eliminates $\Gamma_{11}$,

$$\frac{S_2 RT\omega\tau_{11}^2 C}{\eta_s \eta_{rel} \Gamma} = \frac{\Sigma_{i=1}^{P} C_i}{\Sigma_{i=1}^{P} (C_i/M_i)} \frac{\tau_{11}^2}{\tau_1^2} . \tag{20}$$

The right-hand side of this equation is a molecular weight, so that we can define

$$M_{\tau\Gamma} = \frac{S_2 RT\omega\tau_{11}^2 C}{\eta_s \eta_{rel} \Gamma} = M_1 \frac{\Sigma_{i=1}^{P} C_i}{\Sigma_{i=1}^{P} C_i (M_i/M_1)^{1+2a}} , \tag{21}$$

after substitution of eqs. (6) and (11) for $\tau_{11}^2$ and $\langle\tau_1^2\rangle$, respectively.

Finally, the fourth molecular weight, $M_{\tau A}$, involving the area under a relaxation curve, can be derived from eq. (22) of Klotz and Zimm [20],

$$A/\Gamma = \frac{S_3}{S_2}\frac{\langle\tau_1^3\rangle}{\langle\tau_1^2\rangle}, \tag{22}$$

where $S_3$ is a third constant (see below). We combine eqs. (20) and (22) and obtain

$$\frac{S_3 RT\omega\tau_{11}^3 C}{\eta_s\eta_{rel}A} = \frac{\Sigma_{i=1}^{P} C_i}{\Sigma_{i=1}^{P}(C_i/M_i)}\frac{\tau_{11}^2}{\langle\tau_1^3\rangle}. \tag{23}$$

Multiplying both sides of eq. (23) by $\tau_{11}$ and substituting for $\tau_{11}^3$ and $\langle\tau_1^3\rangle$ from eqs. (6) and (12) yields

$$M_{\tau A} = \frac{S_3 RT\omega\tau_{11}^3 C}{\eta_s\eta_{rel}A} = M_1\frac{\Sigma_{i=1}^{P} C_i}{\Sigma_{i=1}^{P} C_1 (M_i/M_1)^{2+3a}}. \tag{24}$$

It is possible to obtain $M_{\tau\Gamma}$ and $M_{\tau A}$ by direct substitution of eqs. (10), (11), and (12) into (18) and (22). However, intermediate expressions of greater complexity result. These are

$$M_{\Gamma\eta} = \frac{S_1^2 RT\eta_{rel}\Gamma C}{S_2\eta_s\omega\eta_{sp}^2} = \frac{M_{\tau\eta}^2}{M_{\tau\Gamma}}, \tag{25}$$

and

$$M_{A\Gamma\eta} = \frac{S_1 S_2 RTAC}{S_3\eta_s\eta_{sp}\Gamma} = \frac{M_{\tau\eta}^3}{M_{\tau A}M_{\Gamma\eta}}. \tag{26}$$

The formulas for $M_{\tau\eta}$, $M_{\tau\Gamma 11}$, $M_{\tau\Gamma}$, and $M_{\tau A}$ are reproduced in table 4. These molecular weights are not averages since they are not of the form $(\Sigma_{i=1}^{P} C_i M_i^x)/\Sigma_{i=1}^{P} C_i$. They are actually equal to the largest molecular weight raised to the power $(x+1)$ and then divided by the corresponding average. For example eq. (14)

$$M_{\tau\eta} = M_1\frac{\Sigma_{i=1}^{P} C_i}{\Sigma_{i=1}^{P} C_i (M_i/M_1)^a}$$

may be rewritten as

$$M_{\tau\eta} = \frac{M_1^{1+a}}{(\Sigma_{i=1}^{P} C_i M_i^a)/\Sigma_{i=1}^{P} C_i}. \tag{27}$$

$M_{\tau\Gamma}$ and $M_{\tau A}$ have the same form; however, $M_{\tau\Gamma 11}$ is an exception,

$$M_{\tau\Gamma 11} = \frac{M_1^2}{(C_1 M_1)/\Sigma_{i=1}^{P} C_i}, \tag{28}$$

since $(C_1M_1)/\Sigma_{i=1}^{P} C_i$ is not an average molecular weight, but is rather a fraction times $M_1$. Average molecular weights would range between the smallest $M_i$ and $M_1$. Our characteristic molecular weights can be larger than $M_1$, as shown in table 3 for some hypothetical DNA solutions.

### 3.2. Eigenvalue series

The molecular weight equations (13), (21), (24) in the preceding section contain the constants $S_1$, $S_2$, and $S_3$, respectively. Each constant is equal to convergent series, which results from the bead-spring theory of Rouse [24] and Zimm [25], multiplied by a constant $\nu$. For linear molecules $\nu = 1$, and we may write [26],

$$S_1 = \sum_{k=1}^{N}\frac{\lambda_1^*}{\lambda_k^*} = \sum_{k=1}^{N}\frac{\tau_k}{\tau_1}, \tag{29}$$

$$S_2 = \sum_{k=1}^{N}\left(\frac{\lambda_1^*}{\lambda_k^*}\right)^2 = \sum_{k=1}^{N}\left(\frac{\tau_k}{\tau_1}\right)^2, \tag{30}$$

$$S_3 = \sum_{k=1}^{N}\left(\frac{\lambda_1^*}{\lambda_k^*}\right)^2 = \sum_{k=1}^{N}\left(\frac{\tau_k}{\tau_1}\right)^3, \tag{31}$$

where $\lambda_k^*$ is the eigenvalue of the hydrodynamic interaction operator for the $k$th normal mode of motion, and $\tau_k$ is the corresponding relaxation time. Each eigenvalue $\lambda_k^*$, and hence each series, depends upon the extent of hydrodynamic interaction between segments of a randomly coiling chain [27] and upon excluded volume effects [28]. The dependence is expressed as $\lambda_k^* = \lambda_k^*(h, \epsilon)$, where $h$ is a parameter which measures the strength of the interaction and $\epsilon$ accounts for expansion of the coil due to excluded volume. For the bead-spring model, $h$ is given by,

$$h = \frac{2^{\epsilon/2}Nf_0}{(12\pi^3)^{1/2}\eta b N^{(1+\epsilon)/2}}, \tag{32}$$

where $f_0$ is the translational friction coefficient of each bead, $\eta$ is the solvent viscosity, $b$ is the root-mean-square spring length, $N$ is the number of springs

[29]. The two limiting cases for hydrodynamic interaction are $h = 0$, the "free-draining" case with vanishing interaction, and $h = \infty$, the "nondraining" case with dominant interaction. Bloomfield and Zimm [29] considered the nondraining case and obtained

$$S_1 = 2.25, \quad S_2 = 1.146, \quad S_3 = 1.036, \tag{33}$$

for $\epsilon = 0.1$ (which is the value found for native DNA in 0.2 M $Na^+$ neutral buffers [30]). The value of $S_1$ has been used to calculate molecular weights from eq. (13) [4–10]. Dill and Shafer [31] recalculated the eigenvalues of Bloomfield and Zimm more accurately. From their values and eqs. (27)–(29), we found

$$S_1 = 2.211, \quad S_2 = 1.143, \quad S_3 = 1.035. \tag{34}$$

We also determined $S_1$ for $h = \infty$ and $\epsilon = 0.1$ by the method outlined below and found that $S_1 = 2.238$. At the present time we do not know the source of this discrepancy. The experimental results obtained in this work suggested that even the $S_1$ and $S_2$ values in eq. (34) may be too high for T2 DNA (see sect. 5). Since $S_1 = 1.645$ and $S_2 = 1.082$ for the free-draining case (independent of $\epsilon$), we decided to calculate $S_1$ and $S_2$ for T2 DNA considered as a partially free-draining chain with $\epsilon = 0.1$.

The calculation of $S_1$ is accomplished in the following way. First, we determine $h$ from eq. (32). This $h$ is the one which appears in the *approximate* integro-differential equation of Zimm [25]. Osaki [32] has pointed out that the approximate equation is good only for the free-draining or nondraining limits, and not for intermediate degrees of hydrodynamic interaction (with which we are concerned). For the intermediate case, $h$ is replaced by $h_T$ [32–34], where

$$h_T = h/\beta , \tag{35}$$

and

$$\beta = 1 - \frac{4.13\, h}{(1-\epsilon)N^{(1-\epsilon)/2}} . \tag{36}$$

(Osaki [32] and Tschoegl [33] have 4 instead of 4.13 here; the latter comes from a more refined approximation. See Wang [34].) The parameter $\beta$ is called the "free-draining parameter". Once we have calculated $h_T$, we use it to obtain the Flory constant $\Phi$ from table 1, Tschoegl [26], where values of $\Phi(h, \epsilon)$ versus log h are presented. Tschoegl (private communication) has pointed out that $h_T$ may be substituted for $h$ in table 1. Thus, we can obtain $\Phi(h_T, 0.1)$. The series $S_1$ is related to $\Phi$ by combining eq. (29) above and eq. (21) in Tschoegl [26],

$$\Phi(h_T, \epsilon) = N_a \left(1 + \frac{5\epsilon}{12}\right)[100(3\pi)^{1/2}2^{\epsilon/2}]^{-1} \sum_k \frac{h_T}{\lambda_k^*} .$$

$$\sum_k \frac{1}{\lambda_k^*} = \frac{1}{\lambda_1^*} S_1 .$$

Thus,

$$S_1(h_T, 0.1) = 5.066 \times 10^{-22} \frac{\lambda_1^*}{h_T} \Phi(h_T, 0.1) . \tag{37}$$

The eigenvalue $\lambda_1^*(h_T, 0.1)$ may be calculated from the relation [26],

$$\lambda_1^*(h_T, \epsilon) = 1 + \left(\frac{4h_T}{\pi^2}\right)\lambda_1'(\infty, \epsilon) , \tag{38}$$

where $\lambda_1'(\infty, \epsilon) = 5.0076$ [31]. This procedure for determining $S_1$ was necessary since Tschoegl [26] has tabulated values of $\Phi(h, 0.1)$, but not $S_1(h, 0.1)$, versus log $h$.

We begin with the calculation of $h$ from eq. (32). Following the method of Wang and Zimm [35], and Wang [34] we represent the real chain of $N + 1$ segments by $N$ springs between beads located at segment centers, and require that the root-mean-square length $b$ of a spring equal the contour length of a segment $L_c^*$. In order for the model to approximate as closely as possible to the real chain with respect to its contour length and rms end-to-end length, $b$ must be equal to one Kuhn length $b_K$. In this way $N$ is made as large as possible without corresponding to an unrealistic model. Although this method of determining $N$ is arbitrary, the insensitivity of $S_1$ to $h$ (see eq. (45)), and hence to $N$ (eq. (30)), means that an accurate value of $N$ is not required. (See also reference [34].) We calculate $f_0$ by equating it to the segmental friction coefficient for a worm-like chain [36], which we determine from the measured sedimentation coefficient. The sedimentation coefficient of a free molecule equal to one segment in size is

$$S^* = \frac{mL_c^*(1 - \bar{v}\rho)}{N_a f_0} , \tag{39}$$

where $m$ = molecular weight per unit length of DNA, $\bar{v}$ is the partial specific volume of $L_c^*$ in solution, and $\rho$ is the solvent density. If we take $S^* = 6.90 \times$

$10^{-13}$ s$^{-1}$ [37], $m = 195 \times 10^8$ dalton/cm, and $\bar{v}\rho = 0.55$, then the value of $f_0$ is

$$f_0 = 2.111 \times 10^{-2} L_c^* , \tag{40}$$

which can be substituted into eq. (32) to give

$$h = 0.1133 N^{0.45} L_c^*/b . \tag{41}$$

If we choose $b_K = 1300$ Å, then $N = N_K = 473.4$ segments for T2 DNA with $M = 120 \times 10^6$ (average of values from refs. [12] and [13]), and $h = 1.812$. From eqs. (35) and (36), it follows that $h_T = 3.775$. Next, we refer to table 1, Tschoegl [26] and obtain $\Phi(3.775, 0.1) = 1.59 \times 10^{21}$. Substituting these values of $h_T$ and $\Phi$ into eqs. (37) and (38), we arrive at the result

$$S_1(3.775, 0.1) = 2.041 . \tag{42}$$

We choose a simpler method to calculate $S_2$, since it is not as sensitive to variation in $h_T$ as $S_1$ is. Tschoegl [27] presents a table of $S_1$ and $S_2$ values versus $\log h$ for $\epsilon = 0$. We substitute $h_T$ for $h$ in this table and obtain,

$$\frac{S_1(3.775, 0)}{S_1(\infty, 0)} = 0.877, \quad \frac{S_2(3.775, 0)}{S_2(\infty, 0)} = 0.985 . \tag{43}$$

The ratio of $S_2$ values enables us to determine a minimum value for $S_2(3.775, 0.1)$ from $S_2(\infty, 0.1) = 1.143$,

$$S_2(3.775, 0.1) = (0.985)(1.143) = 1.126 . \tag{44}$$

That this is a minimum value can be seen by comparing the $S_1$ ratio in eq. (43) for $\epsilon = 0.1$,

$$\frac{S_1(3.775, 0.1)}{S_1(\infty, 0.1)} = \frac{2.041}{2.211} = 0.923 . \tag{45}$$

The series $S_3$ converges more rapidly than $S_1$ or $S_2$ and, of course, must be greater than 1. Thus, $1 \leqslant S_3(3.775, 0.1) \leqslant S_3(\infty, 0.1) = 1.035$. In view of this and the ratios given in eqs. (43) and (45), we assume

$$S_3(3.775, 0.1) = 1.035 , \tag{46}$$

within about one percent.

## 4. Results

The molecular weight equations presented earlier in this paper (theory) apply to DNA solutions which are infinitely dilute and exhibit Newtonian behavior, i.e., the viscosity coefficient is a constant. In practice neither of these conditions is satisfied — we study solutions of finite concentration, and the viscosity, or rather the specific viscosity, varies with shear rate [21,39] at a given DNA concentration, which is a non Newtonian effect. The other viscoelastic properties would be expected to show this effect [20,40]. The experimental results therefore must be extrapolated to the theoretical conditions — zero concentration and zero shear rate — in order to use these results in the molecular weight equations.

### 4.1. Shear-rate dependence

The specific viscosity of T2 DNA [39] and T4 DN [41] has been shown to depend on shear rate. In both cases, $\eta_{sp}$ increased with decreasing $\kappa$ and at zero shear rate the limiting slope was zero. We have made similar measurements at six different shear stresses, ranging from $2.55 \times 10^{-3}$ to $8.20 \times 10^{-2}$ dyne/cm$^2$ on a series of solutions the concentrations of which ranged from 7 to 30 μg/ml. The results obtained for the shear dependence of $\eta_{sp}$ at three different concentrations are shown in fig. 1.

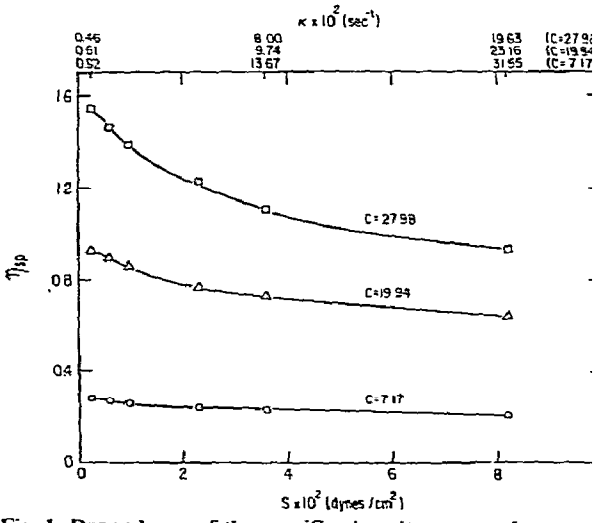


Fig. 1. Dependence of the specific viscosity $\eta_{sp}$ on shear rate or shear stress. The average shear rate $\kappa$ corresponding to a particular average shear stress $S$ and DNA concentration $C$ is given at the top of the graph. The concentrations are expressed in μg DNA/ml.

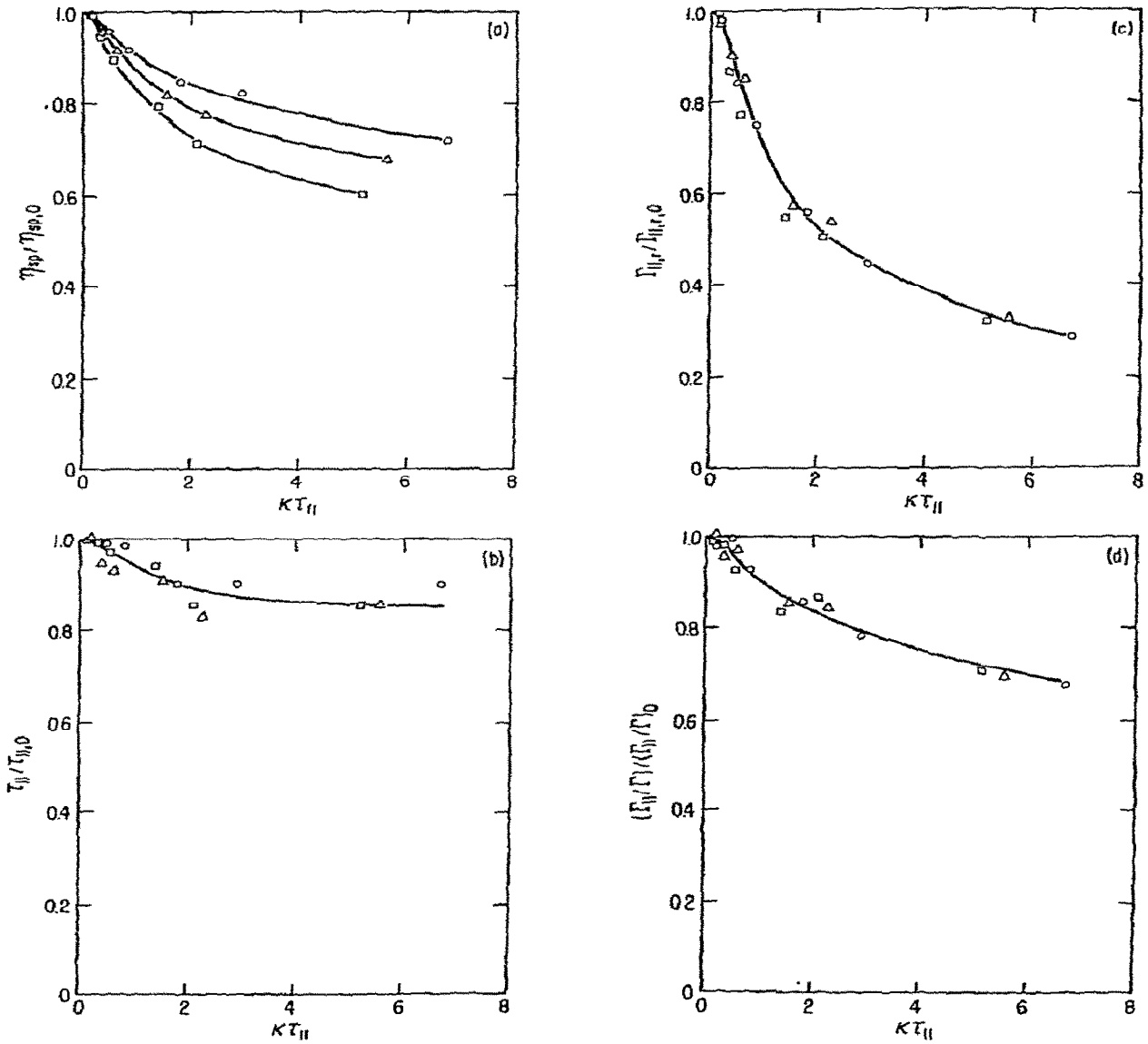


Fig. 2. Dimensionless plots of viscoelastic properties as a function of shear rate. DNA concentrations are denoted by the same symbols as in fig. 1. $\kappa\tau_{11}$ is the shear rate times the measured retardation time for the same run. A subscript "0" refers to the zero shear value. (a) Specific viscosity, $\eta_{sp}$. (b) Principal retardation time, $\tau_{11}$. (c) Reduced, principal recoil amplitude, $\Gamma_{11,r}$. (d) Recoil amplitude ratio, $\Gamma_{11}/\Gamma$.

Table 1
Data obtained at $C = 7.86$ μg DNA/ml [a]

| Run number | $T$ (s/rev) | $\eta_{sp}$ | $\tau_{11}$ (s) | $\Gamma_{11} \times 10^2$ (rad) [c] | $\Gamma \times 10^2$ (rad) [c] | $A \times 10^2$ (rad · s) [c] |
|---|---|---|---|---|---|---|
| 2,8 [b] | 1393.98 | 0.306 | 23.68 | 2.54 | 3.02 | 61.23 |
| 3,9 [b] | 588.18 | 0.298 | 23.24 | 5.09 | 6.26 | 124.95 |
| 4,10 [b] | 353.11 | 0.287 | 22.42 | 7.14 | 9.17 | 169.12 |
| 1,7 [b] | 147.90 | 0.261 | 21.41 | 12.75 | 16.78 | 288.28 |
| 5 | 93.53 | 0.254 | 19.58 | 16.12 | 23.14 | 345.79 |
| 6 | 40.26 | 0.222 | 19.67 | 24.23 | 40.85 | 565.09 |

a) Also presented in fig. 3. See sect. 2 for calculation of $\kappa$ (rad/s) from $T$ (s/rev). See sect. 4 for calculation of $\Gamma_{11,r}$ and $\Gamma_r$ from $\Gamma_{11}$ and $\Gamma$, respectively.
b) Data from both runs were averaged.
c) The units are radians of shear, not radians of rotor rotation.

As suggested by Klotz and Zimm [5], the ratio $\eta_{sp}/\eta_{sp,0}$, where $\eta_{sp,0}$ is the specific viscosity at zero shear rate, may be plotted against the parameter $\kappa\tau_{11}$, which is the *ratio* of a molecule's deforming (shear) rate to its recovery (relaxation) rate. The advantage of this method is that both coordinate axes are dimensionless, and therefore a curve through the experimental points should be independent of DNA size at low concentrations. Fig. 2 (a) presents the data from fig. 1 replotted in this way. Data for T7 DNA, for example, would be expected to fall along this "master" curve. The magnitude of $\kappa\tau_{11}$ is a measure of the molecular deformation. At higher shear rates, increased deformation causes increased alignment of the DNA molecules along fluid streamlines, and thus decreased specific viscosity, as shown in fig. 2 (a). The sensitivity of $\eta_{sp}$ to shear rate decreased with decreasing concentration.

Dimensionless plots for other properties of viscoelastic solutions are also displayed in fig. 2. Since $\Gamma_{11}$ and $\Gamma$ are directly proportional to $\kappa\tau_{11}$, each was divided by the $\kappa\tau_{11}$ value of the same run before extrapolating to zero shear rate (the extrapolation method is described below). $\Gamma_{11}/\kappa\tau_{11} = \Gamma_{11,r}$ and $\Gamma/\kappa\tau_{11} = \Gamma_r$ are themselves dimensionless and are called "reduced" recoil amplitudes ‡. The curves in fig. 2 (b), 2 (c), and 2 (d) appear to be independent of concentration, in contrast to fig. 2 (a) for $\eta_{sp}/\eta_{sp,0}$, although scatter in the data makes an unequivocal interpretation difficult.

From fig. 2 it appears that $\Gamma_{11,r}/\Gamma_{11,r,0}$ was more sensitive to shear rate than $\eta_{sp}/\eta_{sp,0}$, and that $\tau_{11}/\tau_{11,0}$ and $(\Gamma_{11}/\Gamma)/(\Gamma_{11}/\Gamma)_0$ decreased as $\kappa\tau_{11}$ increased to seven. These results would not be expected from the multi-Maxwell-element model of Klotz and Zimm [20]; however, they can be predicted by including a shear-rate dependent viscosity coefficient in a single-element model (see sect. 5).

Typical data obtained in one experiment are presented in table 1. After converting $\Gamma_{11}$ to $\Gamma_{11,r}$ and $\Gamma$ to $\Gamma_r$, we determined the zero-shear values of $\eta_{sp}$, $\tau_{11}$, $\Gamma_{11,r}$, $\Gamma_r$, and $A/\Gamma$ by plotting the natural logarithm of each quantity at a given $\kappa\tau_{11}$ versus $\ln[1 + 3(\kappa\tau_{11})^2]$ (fig. 3). The term $\ln[1 + 3(\kappa\tau_{11})^2]$ was used as the abscissa because, as $\kappa\tau_{11} \to 0$, $\ln[1 + 3(\kappa\tau_{11})^2] \to 3(\kappa\tau_{11})^2$, and, at low $\kappa\tau_{11}$ values, $\eta_{sp}$, $\Gamma_{11,r}$, and $\Gamma_r$ are functions of $(\kappa\tau_{11})^2$ [20,30,39, 40]. The constant 3 is purely empirical [40]. Each double logarithmic plot yielded a set of points which could be fit with a straight line using the method of least squares. Extrapolation of this straight line to zero shear rate was more precise than extrapolation of the curved line which is obtained in the standard plot (fig. 1). The slope and intercept of the least-squares line were calculated for the first three points on each curve. If no consistent curvature of the log-log plot was evident at higher $\kappa\tau_{11}$, all six points were included In fig. 3, all the six points were used to obtain the zero-shear properties $\eta_{sp,0}$, $(\tau_{11}/\eta_{rel})_0$, $\Gamma_{11,r,0}$, and $(A/\Gamma)_0$. We plotted $\ln(A/\Gamma)$ rather than $\ln(A/\kappa\tau_{11})$ because the former is much less shear dependent. The

‡ $\Gamma_r$ is not to be confused with $\Gamma_R$ in ref. [20], which is equal to $\Gamma$ here.

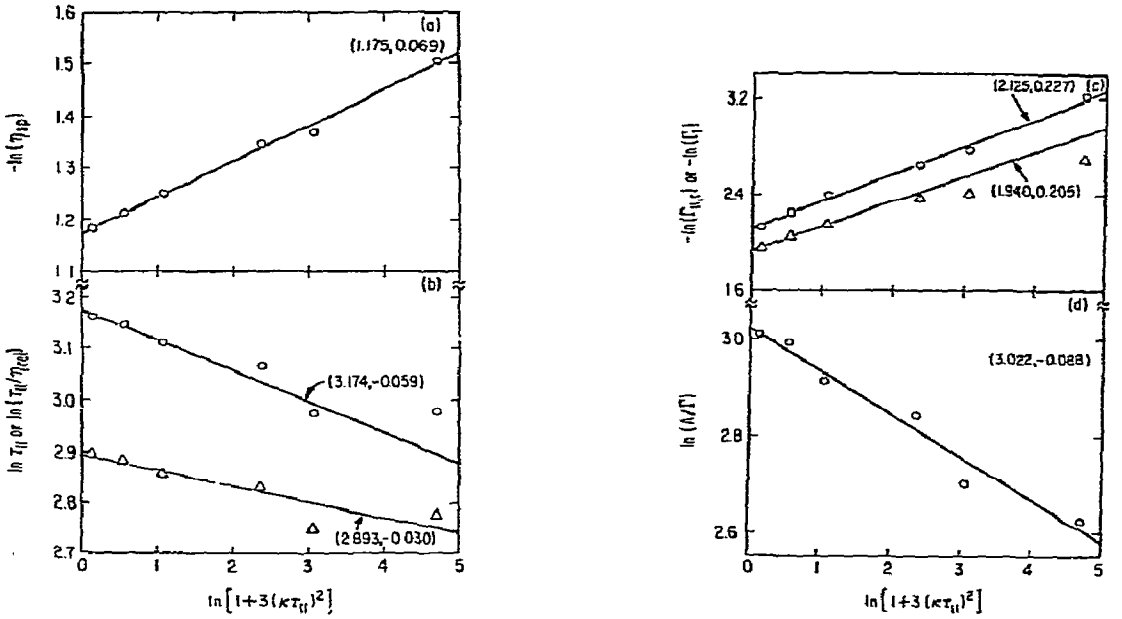


Fig. 3. Double logarithmic plots of viscoelastic properties as a function of shear rate. The data are taken from table 1. Data points were fit to a straight line by the method of least-squares (see Results). The intercept and slope of each line are indicated by a set of two numbers: (intercept, slope). (a) Specific viscosity, $\eta_{sp}$. (b) Principal retardation time, $\tau_{11}$ (s); ratio of the principal retardation time to the relative viscosity, $\tau_{11}/\eta_{rel}$ (s). (○) $\ln(\tau_{11})$; (△) $\ln(\tau_{11}/\eta_{rel})$. (c) Reduced, principal recoil amplitude, $\Gamma_{11,r}$; reduced total recoil amplitude $\Gamma_r$. (○) $-\ln(\Gamma_{11,r})$; (△) $-\ln(\Gamma_r)$. (d) Ratio of the area under the recoil curve to the total recoil amplitude, $A/\Gamma$ (s).

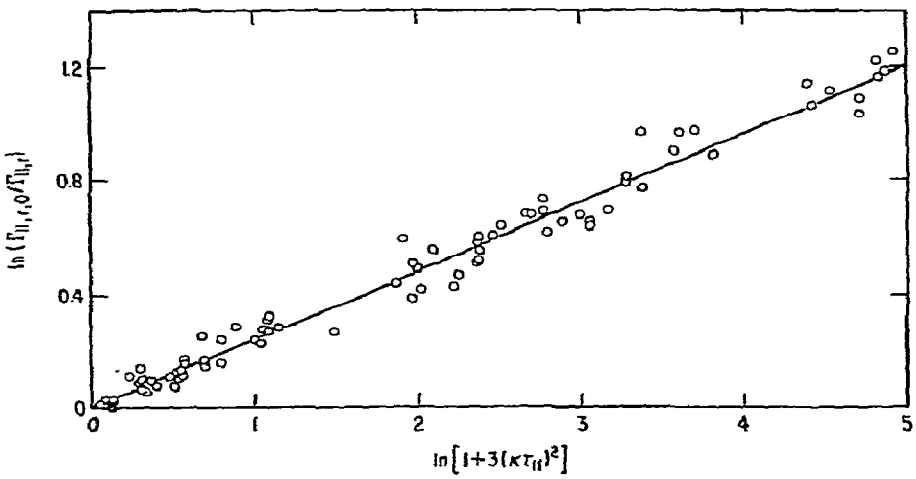


Fig. 4. Double logarithmic plot of the principal recoil amplitude as a function of shear rate. The data points were obtained at eleven concentrations; each point is the average of at least two runs at a given concentration. The slope of the line, 0.241 ± 0.015, is the mean (± the standard deviation of the mean) of all slopes obtained in the manner of fig. 3 (c).

above method of curve fitting was most successful when applied to $\Gamma_{11,r}$. In fig. 4, all of the $\Gamma_{11}$ data which we obtained are displayed as $\ln(\Gamma_{11,r,0}/\Gamma_{11,r})$ versus $\ln[1+3(\kappa\tau_{11})^2]$. The average of the slopes of the individual least-squares lines, such as the one shown in fig. 3 (c), was $0.241 \pm 0.015$. This is the slope of the line drawn in fig. 4; the equation of this line,

$$\ln(\Gamma_{11,r,0}/\Gamma_{11,r} = (0.241 \pm 0.015) \ln[1+3(\kappa\tau_{11})^2], \quad (47)$$

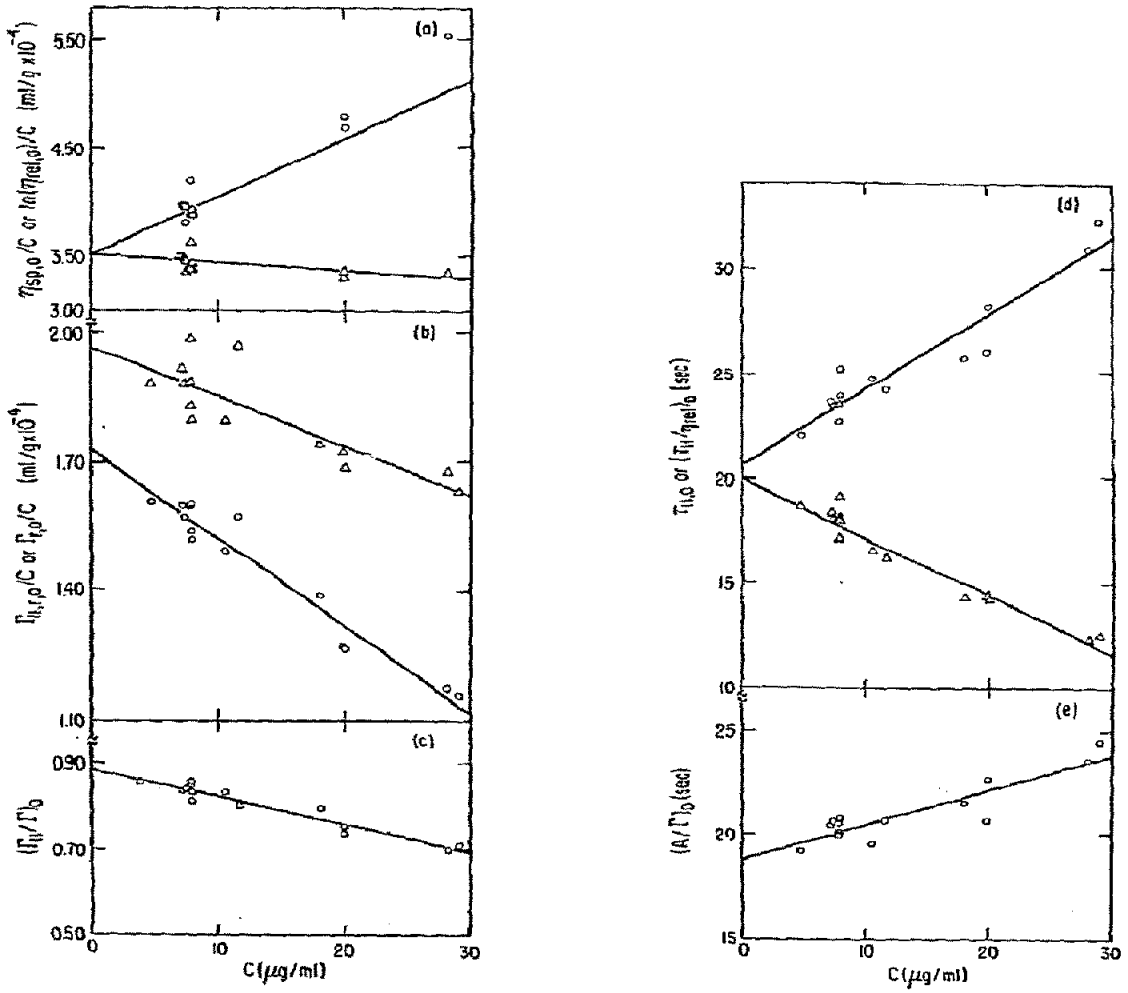


Fig. 5. Dependence of zero-shear, viscoelastic properties on DNA concentration. Each set of data points, except for $\eta_{sp,0}/C$ (see text), was fit with a least-squares straight line. The intercept of the resulting line is presented in table 2. (a) Specific viscosity, $\eta_{sp,0}$; relative viscosity, $\eta_{rel,0}$. (○), $\eta_{sp,0}/C$; (△) $\ln(\eta_{rel,0})/C$. (b) Reduced, pricipal recoil amplitude, $\Gamma_{11,r,0}$; reduced, total recoil amplitude, $\Gamma_{r,0}$. (○) $\Gamma_{11,r,0}$; (△) $\Gamma_{r,0}/C$. (c) Ratio of recoil amplitudes, $(\Gamma_{11}/\Gamma)_0$. (d) Principal retardation time, $\tau_{11,0}$; ratio of the principal retardation time to the relative viscosity, $(\tau_{11}/\eta_{rel})_0$. (○) $\tau_{11,0}$; (△) $(\tau_{11}/\eta_{rel})_0$. (e) Ratio of the area under the recoil curve to the total recoil amplitude, $(A/\Gamma)_0$.

Table 2
Limiting viscoelastic properties of T2 DNA at 25°C [a]

| Limiting property | Value equals intercept from fig. 5 [b] | Hypothetical value in water |
|---|---|---|
| $[\eta_{sp}/C]$ | $(3.51 \pm 0.04) \times 10^4$ ml/g | (same as column 2) |
| $[\Gamma_{11,r}/C]$ [c] | $(1.73 \pm 0.02) \times 10^4$ ml/g | ,, |
| $[\Gamma_r/C]$ [c] | $(1.97 \pm 0.03) \times 10^4$ ml/g | ,, |
| $[\Gamma_{11}/\Gamma]$ | $0.886 \pm 0.009$ | ,, |
| $[\tau_{11}]$ | $20.7 \pm 0.5$ s | $0.85 \pm 0.02$ s [d] |
| $[\tau_{11}/\eta_{rel}]$ | $20.0 \pm 0.5$ s | $0.82 \pm 0.01$ s [d] |
| $[A/\Gamma]$ | $18.8 \pm 0.4$ s | $0.77 \pm 0.02$ s [d] |

a) The viscosity of the glycerol-buffer solvent at 25°C was $\eta_s = (21.71 \pm 0.21) \times 10^{-2}$ poise. The viscosity of water at 25° was assumed to be $\eta_{H_2O} = 0.8913 \times 10^{-2}$ poise [22].
b) The error is the standard deviation obtained from the least-squares formula [45].
c) We define $\Gamma_{11,r} = \Gamma_{11}/\kappa\tau_{11}$ and $\Gamma_r = \Gamma/\kappa\tau_{11}$.
d) The hypothetical value in water is obtained by multiplying the corresponding experimental value in column 2 by the viscosity ratio, 0.8913/21.71.

may perhaps be used to correct $\Gamma_{11,r}$ to zero shear rate for solutions of other DNA molecules. Similarly, for $(\Gamma_{11}/\Gamma)$ we obtained the relation,

$$\ln[(\Gamma_{11}/\Gamma)_0/(\Gamma_{11}/\Gamma)] = (0.063 \pm 0.018) \ln[1 + 3(\kappa\tau_{11})^2] \ . \quad (48)$$

### 4.2. Concentration dependence

The zero-shear properties at various DNA concentrations were subsequently extrapolated to zero concentration (fig. 5). The intercepts in fig. 5 represent the limiting (zero shear rate and zero concentration) viscoelastic properties of T2 DNA in the glycerol-buffer solvent; their values are presented in column 2 of table 2. The limiting properties, by analogy with the limiting viscosity number (or intrinsic viscosity), are bracketed. For example, $[\Gamma_{11,r}/C]$ is the limiting, reduced, principal recoil amplitude, and $[\tau_{11}]$ is the limiting, pricipal retardation time. The slope and intercept of each curve in fig. 5 were determined by least-squares linear regression analysis. In fig. 5 (a), both $\eta_{sp,0}/C$ and $\ln(\eta_{rel,0})/C$ were plotted as functions of $C$. We found, as did Crothers and Zimm [39] that the logarithmic plot was more nearly linear and thus was preferable to the specific viscosity plot in determining $[\eta_{sp}/C]$. The slope of the regression line for the logarithmic plot was $-0.74 \times 10^9$ (ml/g)$^2$. From this, we calculated the slope of the limiting line for the specific viscosity plot and the Huggin's constant, $k' = 0.44$ (see ref. [40] for details).

The dependence of the ratio $(\Gamma_{11}/\Gamma)_0$ on concentration is shown in fig. 5 (c). The limiting value, $[\Gamma_{11}/\Gamma] = 0.886 \pm 0.009$, obtained from this plot is approximately the same as the theoretical value 0.888 (table 3) for a homogeneous solution. In table 3 we have made theoretical calculations illustrating the effect of DNA size heterogeneity on certain properties. As can be seen from the table, a hypothetical DNA solution containing 5% half-size and 95% full-size molecules would have $[\Gamma_{11}/\Gamma] = 0.879$, within one standard deviation of the experimental result. Thus, our solutions could contain a small fraction of half-size molecules. Table 3 also indicates that a larger fraction of one-tenth size molecules could be present in our solutions (see sect. 5).

The quantities $\tau_{11,0}$ and $(\tau_{11}/\eta_{rel})_0$ in fig. 5 (d) should approach the same value at zero concentration. They did, within error limits of two standard deviations, as shown in table 2. We used the value of $[\tau_{11}/\eta_{rel}] = 20.0$ s in calculations of molecular weight because it had a lower standard deviation than $[\tau_{11}]$. The concentration dependence of $(A/\Gamma)_0$ is less than that of $\tau_{11,0}$ or $(\tau_{11}/\eta_{rel})_0$ (fig. 5 (d) and (e)), and the limiting value of $[A/\Gamma] = 18.8$ s (table 2). If we divide $[A/\Gamma]$ by $[\tau_{11}/\eta_{rel}]$, we obtain $0.94 \pm 0.02$ which is close to the theoretical value 0.919 (table 3) for a homogeneous solution. Theoretical values of $A/\Gamma\tau_{11}$, for hypothetical heterogeneous DNA solutions, are given in table 3.

Characteristic molecular weights were calculated from the corresponding properties (table 2) by the equations derived earlier (sect. 3). The results are presented in table 4.

## 5. Discussion

The primary new results of this work are (1) the demonstration of changes in viscoelastic properties of DNA solutions with variations in steady-state shear rate $\kappa$, and (2) the calculation of a molecular weight for T2 NaDNA from several viscoelastic properties, which have been extrapolated to zero shear rate and

Table 3
Effect of DNA size heterogeneity on viscoelastic properties and characteristic molecular weights – predictions from theory

| $M_2/M_1$ | $C_1/C$ | $C_2/C$ | $\frac{\eta_{sp}/C}{(\eta_{sp}/C)_1}$ | $\Gamma_{11}/\Gamma$ | $A/\Gamma\tau_{11}$ | $M_1/M_\tau\Gamma_{11}$ | $M_1/M_{\tau\eta}$ |
|---|---|---|---|---|---|---|---|
| – | 1.00 | 0 | 1.000 | 0.888 ($=1/S_2$) | 0.919 ($=S_3/S_2$) | 1.000 | 1.000 |
| 0.50 | 0.95 | 0.05 | 0.982 | 0.879 | 0.913 | 0.950 | 0.982 |
| „ | 0.90 | 0.10 | 0.963 | 0.869 | 0.906 | 0.900 | 0.963 |
| „ | 0.80 | 0.20 | 0.926 | 0.846 | 0.889 | 0.800 | 0.926 |
| „ | 0.50 | 0.50 | 0.815 | 0.741 | 0.815 | 0.500 | 0.815 |
| 0.10 | 0.90 | 0.10 | 0.922 | 0.888 | 0.919 | 0.900 | 0.922 |
| „ | 0.80 | 0.20 | 0.843 | 0.887 | 0.918 | 0.800 | 0.843 |
| „ | 0.50 | 0.50 | 0.608 | 0.884 | 0.915 | 0.500 | 0.698 |

In this table, we consider hypothetical DNA solutions composed of two species, 1 and 2, whose sizes are $M_1$ and $M_2$, respectively. The total DNA concentration is the sum of the concentrations of the two species, $C = C_1 + C_2$. From eqs. (5) and (9) in sect. 3a, we obtain

$$\frac{\eta_{sp}/C}{(\eta_{sp}/C)_1} = \frac{\Sigma_{i=1}^{p} C_i (M_i/M_1)^a}{\Sigma_{i=1}^{p} C_i} = C_1/C + C_2/C\,(M_2/M_1)^a$$

where $(\eta_{sp}/C)_1$ is the limiting viscosity number of species 1. This equation enables us to calculate the numbers in column 4, if we assume $a = 0.665$ [39]. Similarly, eqs. (6), (11), and (19) yield (for $\nu = 1$)

$$\frac{\Gamma_{11}}{\Gamma} = \frac{C_1}{S_2\,\Sigma_{i=1}^{p} C_i (M_i/M_1)^{1+2a}} = \frac{1}{S_2}\{1 + C_2/C_1\,(M_2/M_1)^{1+2a}\}^{-1}$$

from which column 5 results. The numbers in column 6 are calculated from the equation,

$$\frac{A}{\Gamma\tau_{11}} = \frac{S_3}{S_2}\,\frac{\Sigma_{i=1}^{p} C_i (M_i/M_1)^{2+3a}}{\Sigma_{i=1}^{p} C_i (M_i/M_1)^{1+2a}} = \frac{S_3}{S_2}\,\frac{1 + C_2/C_1 (M_2/M_1)^{2+3a}}{1 + C_2/C_1 (M_2/M_1)^{1+2a}},$$

which is derived from eqs. (6), (11), (12), and (22). The molecular weight ratios are obtained from column 3, table 4. The purpose of these calculations is to indicate the sensitivity of certain viscoelastic properties and characteristic molecular weight to DNA size heterogeneity. The theoretical values presented in column 5 and 6 may be compared to the experimental results for $[\Gamma_{11}/\Gamma]$ and $[A/\Gamma]/[\tau_{11}]$, respectively (see sect. 4). Note that the viscoelastic properties from the theory refer to the condition of infinite dilution and Newtonian behavior.

zero concentration.

The specific viscosity is the only viscoelastic property of T2 DNA solutions which has previously been shown to depend on $\kappa$. Crothers and Zimm [21,39] showed that the shape of the curve of $\eta_{sp}/\eta_{sp,0}$ is concave downward at low shear rates and upward at higher shear rates. The point of the inflection is around $\kappa\tau_{11} \simeq 0.3$ (assuming $\tau_{11} \simeq 0.7$ s for T2 DNA in BPES, which was the solvent used in their work). The curves in fig. 1 and 2 (a) are very similar to those of Crothers and Zimm, but since our lowest $\kappa\tau_{11}$ was 0.14 compared with their lowest value of about 0.02, the initial downward curvature is not as apparent. On the basis of theoretical arguments [40], though, an approximately parabolic curve shape at low $\kappa\tau_{11}$ and a slope equal to zero at $\kappa\tau_{11} = 0$ are required. These considerations also guided our choice of an extrapolation procedure, i.e. – ln $\eta_{sp}$ versus ln$[1 + 3(\kappa\tau_{11})^2]$, from which we obtained $\eta_{sp,0}$.

Our result for the limiting viscosity number of T2 DNA is $(3.51 \pm 0.04) \times 10^4$ ml/g. This is larger than $3.16 \times 10^4$ ml/g reported by Crothers and Zimm [39]. A direct comparison is not possible, though, because the conditions of measurement were different in each case: (1) our solvent contained glycerol while theirs did not; and (2) the $Na^+$ concentration in our solvent was 0.06 M while theirs was 0.2 M. We can correct for the difference in $Na^+$ concentration with eq. (5) of Ross and Scruggs [42]. In 0.2 M $Na^+$, our result becomes $(3.51 \times 10^4)\,(0.883) = 3.10 \times 10^4$ ml/g.

Table 4
Characteristic molecular weights for T2 NaDNA

| Molecular weight | Formula for molecular weight | Equivalent statistical formula | Formula of column 2 with limiting viscoelastic properties | $(M \pm \sigma) \times 10^{-6}$ calculated from previous column [b] |
|---|---|---|---|---|
| $M_{\tau\Gamma_{11}}$ | $\frac{\nu RT\omega\tau_{11}^2 C}{\eta_s\eta_{rel}\Gamma_{11}}$ | $M_1 \frac{\Sigma C_i}{C_1}$ | $\frac{\nu RT}{\eta_s} \frac{[\tau_{11}/\eta_{rel}]}{[\Gamma_{11,r}/C]}$ | 131.9 ± 2.8 |
| $M_{\tau\eta}$ | $\frac{S_1 RT\tau_{11} C}{\eta_s\eta_{sp}}$ | $M_1 \frac{\Sigma C_i}{\Sigma C_i(M_i/M_1)^a}$ | $\frac{S_1 RT}{\eta_s} \frac{[\tau_{11}/\eta_{rel}]}{[\eta_{sp}/C]}$ [a] | 132.7 ± 2.8 |
| $M_{\tau\Gamma}$ | $\frac{S_2 RT\omega\tau_{11}^2 C}{\eta_s\eta_{rel}\Gamma}$ | $M_1 \frac{\Sigma C_i}{\Sigma C_i(M_i/M_1)^{1+2a}}$ | $\frac{S_2 RT}{\eta_s} \frac{[\tau_{11}/\eta_{rel}]}{[\Gamma_r/C]}$ | 130.5 ± 3.1 |
| $M_{\tau A}$ | $\frac{S_3 RT\omega\tau_{11}^3 C}{\eta_s\eta_{rel}A}$ | $M_1 \frac{\Sigma C_i}{\Sigma C_i(M_i/M_1)^{2+3a}}$ | $\frac{S_3 RT}{\eta_s} \frac{[\tau_{11}/\eta_{rel}]^2}{[A_r/C]}$ [a] | 127.6 ± 5.4 [c] |
| | | | | Mean = 130.7 ± 1.6 [d] |

a) At $C = 0$, $\tau_{11,0}$ and $(\tau_{11}/\eta_{rel})_0$ have the same value (see text).
b) $\sigma$ is the standard deviation.
c) The value of $M_{\tau A}$ was calculated from the equation, $M_{A\Gamma\eta} = (S_1S_2RT/S_3\eta_s)[A/\Gamma]/[\eta_{sp}/C] = (135.7 \pm 3.5) \times 10^6$, and the relation $M_{\tau A} = M_{\tau\eta}M_{\tau\Gamma}/M_{A\Gamma\eta}$ (see sect. 3a).
d) The error given here is the average deviation of the four $M$'s about their mean value.

Apparently, the presence of glycerol does not affect the T2 DNA coil dimensions significantly.

Our limiting viscosity number is also greater than the value of $3.05 \times 10^4$ obtained by Chapman et al. [4] (reported again in ref. [5]) for T2 DNA in glycerol-BBES buffer ($\eta_s = 22.0$ cp). We believe the discrepancy is due to the shear-rate dependence of $\eta_{sp}$. Chapman et al. made measurements at average shear stresses of 2 to $50 \times 10^{-2}$ dyne/cm$^2$ while ours ranged from 0.255 to $8.20 \times 10^{-2}$ dyne/cm$^2$ (fig. 1). Because we obtained more data at lower shear stresses (or rates), we were able to make a better extrapolation of $\eta_{sp}$ to zero shear rate (fig. 3 (a)), and hence obtained higher values of $\eta_{sp,0}$ and $[\eta_{sp}/C]$. Our range of DNA concentrations encompasses that of Chapman et al., which was 10 to 22 $\mu$g/ml.

The retardation time $\tau_{11}$ exhibited an apparent shear-rate dependence. The dependence may be predicted from a single-Maxwell-element model [4] of a viscoelastic solution, if the Maxwell-element dashpot viscosity is allowed to vary with shear-rate [40]. The equation of rotor motion obtained for this modified model may be displayed as a semi-log plot of rotor angle versus time during creep recovery. The plot is straight only when the steady-state rate approaches zero. At higher shear rates, the semi-log plot is curved, and when one attempts to fit the curve with a straight line within a finite range of time, the slope of this line (which is equal to the apparent value of $-1/\tau_{11}$) is greater than the true limiting slope. Hence, at values of $\kappa$ greater then zero, the apparent $\tau_{11}$ is less than the true $\tau_{11}$. As shown in fig. 2 (b), we found that $\tau_{11}$ appeared to decrease about 15% between $\kappa\tau_{11} = 0$ and $\kappa\tau_{11} = 7$. Chapman et al considered $\tau_{11}$ to be independent of shear rate within their experimental error, but this was larger than ours.

The values for the limiting retardation time, expressed as $[\tau_{11}]$ or $[\tau_{11}/\eta_{rel}]$, were 20.7 ± 0.5 s and 20.0 ± 0.3 s (see table 2). Within error limits, these are the same; we prefer the latter value for calculations of molecular weight because it has a smaller standard deviation. When $[\tau_{11}/\eta_{rel}]$ is corrected to water (see table 2), its value is [‡]

$$[\tau_{11}/\eta_{rel}]_w = [\tau_{11}]_w = 0.82 .$$

The $[\tau_{11}]_w$ reported by Chapman et al. is 0.57 s, 30%

‡ In 0.2 M $Na^+$, the limiting retardation time would be $[\tau_{11}]_w = (0.82)(0.883) = 0.72$ s (see discussion of limiting viscosity number above).

lower than our value. Since their shear rates were greater than ours, a lowering of $[\tau_{11}]_w$ by at least 15% might be expected; our improvement of the signal to noise ratio for the recoil curves [23], allowing more accurate measurement at longer times, could account for some of the discrepancy. Ken Dill (unpublished results) has recently measured relaxation and retardation times of T2 DNA and obtained the same $[\tau_{11}]_w$ as we have.

Values for the limiting, reduced recoil amplitudes, $[\Gamma_{11,r}/C]$ and $[\Gamma_r/C]$, have not been reported previously. We find that $\Gamma_{11,r}$ and $\Gamma_r$ depend on shear rate, and in fact, they decrease more rapidly with increasing $\kappa\tau_{11}$ than does $\eta_{sp}$ (fig. 2 (a), (c), and (d)). Also, $\Gamma_{11,r}$ decreases more rapidly than $\Gamma_r$, and consequently $\Gamma_{11}/\Gamma$ is lower at higher $\kappa\tau_{11}$ (fig. 2 (d)). We have been able to mimic the shear-rate dependence of $\Gamma_r$ with the same single–Maxwell-element model mentioned above [40]. To mimic the shear-rate dependence of $\Gamma_{11}/\Gamma$ would require extension of this single-element model to a multi-element model in which the viscosity coefficient $\eta_i$ of *each dashpot* varies with shear rate. Since $\eta_i$ actually depends on shear rate times relaxation time [30,40] and not just shear rate alone, $\eta_1$ would decrease more rapidly than $\eta_2$, $\eta_3$, ..., as shear rate increases. Correspondingly, $\Gamma_{1,r}$ which is proportional to $\eta_1$ would also decrease more rapidly than $\Gamma_r$ which is related to the sum of all the $\eta_i$'s [40]. This prediction is in agreement with the experiemtnal observations. The model is somewhat more complicated for a heterogeneous population of DNA molecules. Even so, the amplitude of the *longest* mode for the largest molecules $\Gamma_{11,r}$ would be more sensitive to shear than the total amplitude $\Gamma_r$.

If our results on shear effects are to be applied to other DNA solutions, some caution is necessary. The data for the master curve in fig. 4, and the empirical equations (47) and (48), were obtained over a limited range of $\kappa\tau_{11}$ values, and the T2 DNA solutions appeared to be nearly homogeneous (see below). These data can be used directly to correct for shear rate dependence in other DNA solutions in which there is little heterogeneity. If significant heterogeneity exists, though, these data provide only a maximum correction. For example, we consider the results of Uhlenhopp, Zimm, and Cummings [7] on aberrant T2. If we extrapolate our data to the high $\kappa\tau_{11}$ reported in their experiments, then we can correct their values of $\Gamma_{11,r} = 0.80$ and $\Gamma_{11}/\Gamma = 0.35$ at $\kappa\tau_{11} = 22.80$ (our calculation of $\kappa\tau_{11}$ from their data) to $\kappa\tau_{11} = 0$. From eqs. (47) and (48) above, the maximum zero-shear values would be $\Gamma_{11,r,0} = 4.70$ and $(\Gamma_{11}/\Gamma)_0 = 0.56$. These corrections are significant because the zero-shear values, when extrapolated to zero concentration, would give a lower molecular weight (column 4, table 4) and a higher $[\Gamma_{11}/\Gamma]$ than were reported. A higher $[\Gamma_{11}/\Gamma]$ would imply less heterogeneity in DNA size (see column 5, table 3).

The concentration dependence of $\Gamma_{11,r,0}/C$ and $\Gamma_{r,0}/C$ presented in fig. 5 (b) is in qualitative agreement with the phenomelological theory of Holmes, Ninomiya, and Ferry [43]. They predict that $J_e/C$, where $J_e$ is the steady-state compliance, decreases with increasing concentration,

$$\frac{J_e/C}{(J_e/C)_{C\to 0}} = \left(1 + \frac{C[\eta_{sp}/C]}{\sqrt{2}}\right)^{-2} . \tag{49}$$

It is possible to show from the definitions of $J_e$, $\Gamma$, and $\Gamma_r$ that

$$J_e = \frac{\Gamma}{\eta_s \eta_{rel} \kappa} = \Gamma_r \left(\frac{\tau_{11}}{\eta_s \eta_{rel}}\right). \tag{50}$$

Thus, $\Gamma_{r,0}/C$ might also be expected to decrease with concentration. In order to make a quantative comparison, it is necessary to recognize that $(\tau_{11}/\eta_{rel})_0$ decreases with increasing concentration. From fig. 5, we can calculate that for $C = 10$ μg/ml,

$$\frac{\Gamma_{r,0}/C}{[\Gamma_r/C]} \times \frac{(\tau_{11}/\eta_{rel})_0}{[\tau_{11}/\eta_{rel}]} = (0.94)(0.86) = 0.81 , \tag{51}$$

while the decrease predicted from eq. (49) would be

$$\frac{J_e/C}{(J_e/C)_{C\to 0}} = 0.64 , \tag{52}$$

where $[\eta_{sp}/C]$ is taken from table 2. Since $(J_e/C)/(J_e/C)_{C\to 0}$ is less than $(\tau_{11}/\eta_{rel})_0/[\tau_{11}/\eta_{rel}]$ at $C = 10$μg/ml, it seems likely that $(\Gamma_{r,0}/C)/[\Gamma_r/C]$ should also decrease with increasing concentration, as we in fact observed. Comparison of eqs. (51) and (52) indicates that there is qualitative agreement between the concentration dependence observed for $\Gamma_{r,0}/C$ and $(\tau_{11}/\eta_{rel})_0$ and that predicted from the phenomenological theory.

As shown in fig. 5 (c), we found that the zero-shear ratio of recoil amplitudes $(\Gamma_{11}/\Gamma)_0$ also decreased with increasing concentration. A similar effect was observed

by Klotz and Zimm [5] for E. coli lysates at finite shear rates.

In table 4 we present the characteristic molecular weights calculated from the limiting viscoelastic properties of T2 NaDNA: $M_{\tau\Gamma_{11}} = 131.9$, $M_{\tau\eta} = 132.7$, $M_{\tau\Gamma} = 130.5$, and $M_{\tau A} = 127.6 \times 10^6$. The mean of these values is $(130.7 \pm 1.6) \times 10^6$. Errors in DNA concentration determination are *not* included in the average deviation (see below). Because of this, the small average deviation actually refers to the mean of $M_{\tau\Gamma_{11}}/C$, $M_{\tau\eta}/C$, and $M_{\tau A}/C$, obtained at a given concentration $C$. We did not calculate these quantities specifically, but could do so from the available data. We will now show that these quantities are related to the number of DNA molecules per unit volume and that this is what we have determined accurately. Consider the formulas in columns 2 and 3, table 4. For $M_{\tau\Gamma_{11}}$,

$$\frac{M_{\tau\Gamma_{11}}}{C} = \frac{RT\omega\tau_{11}^2}{\eta_s\eta_{rel}\Gamma_{11}} = \frac{M_1}{C_1} = \frac{N_a}{L_1}, \tag{53}$$

where $L_1$ = the number of molecules of species 1 per unit volume (see sect. 3a) and $N_a$ = Avogadro's number. Rearranging this equation, we can define $L_{\tau\Gamma_{11}}$ as

$$L_{\tau\Gamma_{11}} = \frac{N_a\eta_s\eta_{rel}\Gamma_{11}}{RT\omega\tau_{11}^2} = L_1 = N_a\frac{C}{M_{\tau\Gamma_{11}}}. \tag{54}$$

For $M_{\tau\eta}$, we define

$$L_{\tau\eta} = N_a\left\{\frac{\Sigma\, C_i(M_i/M_1)^a}{M_i}\right\} = N_a\frac{C}{M_{\tau\eta}}. \tag{55}$$

Comparable equations are obtained for $L_{\tau\Gamma}$ and $L_{\tau A}$. Our measurements at a given DNA concentration, then, enable us to calculate the number of molecules per unit volume in different ways. The small average deviation for $L_{\tau\Gamma_{11}}$, $L_{\tau\eta}$, $L_{\tau\Gamma}$, and $L_{\tau A}$ suggests (1) that the theoretical equations we have used are valid, and (2) that our T2 DNA solutions are nearly homogeneous. (We note that $M_{\tau\Gamma_{11}}$, $M_{\tau\eta}$, $M_{\tau\Gamma}$, and $M_{\tau A}$ could have been obtained from the intercepts of concentration plots of $L_{\tau\Gamma_{11}}/C$, etc.)!

In order to estimate the extent of DNA size heterogeneity in our solutions, we made the following calculations. Assume that a DNA solution contains two species, 1 and 2, with concentrations $C_1$ and $C_2$. Species 2 is one-half the size of species 1, so that $M_2/M_1 = 0.5$. From table 4, we can write

$$H_{\Gamma_{11}\eta} = \frac{M_{\tau\eta}}{M_{\tau\Gamma_{11}}} = \left[1 + \frac{C_2}{C_1}\left(\frac{M_2}{M_1}\right)^a\right]^{-1} = 1.00 \pm 0.02,$$

$$H_{\Gamma_{11}\Gamma} = \frac{M_{\tau\Gamma}}{M_{\tau\Gamma_{11}}} = \left[1 + \frac{C_2}{C_1}\left(\frac{M_2}{M_1}\right)^{1+2a}\right]^{-1} = 1.00 \pm 0.01$$

$$H_{\Gamma_{11}A} = \frac{M_{\tau A}}{M_{\tau\Gamma_{11}}} = \left[1 + \frac{C_2}{C_1}\left(\frac{M_2}{M_1}\right)^{2+3a}\right]^{-1} = 0.98 \pm 0.03$$

where the $H$'s are called "heterogeneity indices". The error (one standard deviation) presented is that resulting from viscoelastic measurements alone, since the concentration terms in the molecular weight formulas have cancelled out (i.e., $M_{\tau\eta}/M_{\tau\Gamma_{11}} = L_{\tau\Gamma_{11}}/L_{\tau\eta}$). When we include this error, the values of $C_2/C_1$ which we calculate range from 0 to 0.03 for $H_{\Gamma_{11}\eta}$, from 0 to 0.05 for $H_{\Gamma_{11}\Gamma}$, and from 0 to 0.84 for $H_{\Gamma_{11}A}$. The index $H_{\Gamma_{11}\eta}$ is the most sensitive to heterogeneity, and so we consider it to be the most reliable number from which to calculate $C_2/C_1$. Thus, within the above error limits, our DNA solutions contain less than 3% (from $H_{\Gamma_{11}\eta}$), or perhaps 5% (from $H_{\Gamma_{11}\Gamma}$), half-size molecules, with the most probable value being zero ($H_{\Gamma_{11}\eta} = H_{\Gamma_{11}\Gamma} = 1.00$). It appears that $H_{\Gamma_{11}A}$ is quite insensitive to the presence of half-size molecules.

A similar analysis is possible for the case in which species 2 is one-tenth the size of species 1. In this case, the range of $C_2/C_1$ values is 0 to 0.06 for $H_{\Gamma_{11}\eta}$ and 0 to 2.60 for $H_{\Gamma_{11}\Gamma}$. We have ruled out, though, the presence of more than 2% by weight of small fragments (e.g., one-tenth size molecules) by electron microscopic examination of our solutions (Ruth Kavenoff and Brian Bowen, unpublished observations). Most of our data therefore indicate that the fraction of intact T2 DNA molecules in our solutions is at least 93% by weight.

If the percentage of intact molecules is less than 100%, then our characteristic molecular weights will each be larger than the true molecular weight $M_1$. This is illustrated in table 3, where we have calculated the ratios $M_1/M_{\tau\Gamma_{11}}$ and $M_1/M_{\tau\eta}$ from the formulas in table 4. As pointed out earlier, though, the most probable value of $C_2/C_1$ is zero. Thus, the most probable value for the molecular weight of T2 DNA is $(130.7 \pm 1.6) \times 10^6$, considering the sources of error discussed so far.

We can compare this value directly to the molecular

weight obtained by Chapman et al. [4] since they used the same extinction coefficient as we did to determine T2 DNA concentration (see below). They obtained $[\tau_{11}]_w = 0.57$ s and $[\eta_{sp}/C] = 3.05 \times 10^4$ ml/g, as discussed above, and calculated essentially $M_{\tau\eta}$, using $S_1 = 2.225$ (see sect. 3.2). Their result, $M_{\tau\eta} = 115 \times 10^6$, is lower than ours, probably for reasons mentioned earlier.

As described in sect. 3.2, we have recalculated $S_1$ and $S_2$, assuming T2 DNA to be a partially free-draining chain. The results $S_1 = 2.041$ and $S_2 = 1.126$ were used to calculate $M_{\tau\eta} = 132.7 \times 10^6$ and $M_{\tau\Gamma} = 130.5 \times 10^6$, respectively. The agreement between these two $M$'s, and among all four $M$'s, suggest that in viscoelastic experiments T2 DNA behaves as a partially free-draining chain molecule.

Finally, we assess the error associated with the determination of DNA concentrations. Typically, concentrations of DNA in our stock solutions were determined by absorbance and then quantitative dilutions were made by weighing (see sect. 2). The average error in the weight and absorbance measurements, though, may have been consistently too high, because of the presence of residual protein in our extracts. For the three stock solutions studied, the absorbance ratio $A_{260}/A_{280}$ was 1.72, 1.72, 1.78. These are less than 1.839, reported by Felsenfeld and Hirschman [44] for purified P. mirabilis DNA which has 38% GC base pairs compared to 35% for T2 [22]. If we assume that $E^{1\%}_{260}(\text{DNA})/E^{1\%}_{280}(\text{DNA}) = 1.839$, $E^{2\%}_{260}(\text{protein}) = E^{1\%}_{280}(\text{protein}) = E^{1\%}_{280}(\text{T4 lysozyme}) = 12.8$ [?], and $E^{1\%}_{260}(\text{DNA}) = 181$ [19], then $A^{true}_{260}/A^{obs}_{260} = 0.932$. This is the maximum correction because in general $E^{1\%}_{260}(\text{protein}) < E^{1\%}_{280}(\text{protein})$. The average correction would be $0.966 \pm 0.039$, including weighing errors. Multiplying this by $(130.7 \pm 1.6) \times 10^6$ lowers the molecular weight to $(126 \pm 5) \times 10^6$.

In table 5 we compare our result with some of the more recent values for T2 and T4 DNA molecular weights, determined by other techniques (T4 DNA is expected to be larger than T2 DNA by about 2%, due to differences in glucosylation [14]). It is apparent from this table that our mean molecular weight is within the range of these reported values.

We are able to draw several conclusions from our results. Viscoelastic properties of DNA solutions, measured under conditions of steady state shearing, depend on the shear rate $\kappa$. When these properties are extrapolated to zero shear rate and zero concentration, limiting values are obtained which can be used to calculate characteristic molecular weights. For T2 DNA, the characteristic $M$'s agree very well *with each other*

Table 5
Reported values for T2 and T4 DNA molecular weights

| Observer | Method | Bacteriophage | $M \times 10^6$ |
|---|---|---|---|
| Schmid and Hearst [11] | Density gradient sedimentation equilibrium | T4 | 113.5 ± 6 a) |
| Leighton and Rubenstein [12] | $^{32}P$ star counting (autoradiography) | T2 | 132 ± 12 |
| Dubin et al. [13] | Sedimentation-diffusion of phage | T4 | 105.7 ± 3.8 |
| Lang [14] | Electron microscopy | T4<br>(T2) | 119 ± 2<br>(116 ± 2) b) |
| Weissman et al. [15] | Fluctuation spectroscopy | T2 | 114 ± 5 |
| This paper | Viscoelasticity | T2 | 126 ± 5 (130.7 ± 1.6 c)) |

a) The original value of Schmid and Hearst has been increased by 7.4%, as reported by Freifelder [46].
b) Both values were calculated from the measured length of T4 DNA. Different mass/length factors are due to glucosylation.
c) Value without allowance for concentration uncertainty (see sect. 5).

suggesting (1) that the theoretical equations from which the $M$'s (or $L$'s) are calculated are internally consistent, (2) that T2 DNA behaves as a partially free-draining chain, and (3) that our solutions are nearly homogeneous in DNA size. When the error involved in DNA concentration measurements is considered, the mean of the characteristic $M$'s is lowered and their average deviation increased. The resultant molecular weight, $(126 \pm 5) \times 10^6$, is slightly larger than most of the previously reported values, but still in good agreement with them.

## Acknowledgements

We wish to thank Ruth Kavenoff for preparing T2 DNA samples for electron microscopy, Ken Dill for providing us with his unpublished results, and Lynn Klotz for helpful comments. This research was funded by grant GM-11916 from the U.S. National Institutes of Health. During this work, B.C.B. was supported by a U.S. National Institutes of Health predoctoral traineeship (USPHS 2-T01-GM-01045).

## References

[1] T. Alfrey Jr., Mechanical behavior of high polymers, [Interscience Publishers, Inc., New York, 1948).
[2] J.D. Ferry, Viscoelastic properties of polymers (2nd. Ed., John Wiley and Sons, Inc., New York, 1970).
[3] J.J. Aklonis, W.J. MacKnight and M. Shen, Introduction to polymer viscoelasticity (Wiley-Interscience, New York, 1972).
[4] R.E. Chapman Jr., L.C. Klotz, D.S. Thompson and B.H. Zimm, Macromolecules 2 (1969) 637.
[5] L.C. Klotz and B.H. Zimm, J. Mol. Biol. 72 (1972) 779.
[6] R. Kavenoff and B.H. Zimm, Chromosoma 41 (1973) 1.
[7] E.L. Uhlenhopp, B.H. Zimm and D.J. Cummings, J. Mol. Biol. 89 (1974) 689.
[8] E.L. Uhlenhopp and B.H. Zimm, Biophys. J. 15 (1975) 223.
[9] G.D. Lauer and L.C. Klotz, J. Mol. Biol. 96 (1975) 309.
[10] T.H. Roberts, L.C. Klotz and A.R. Loeblich, III, J. Mol. Biol., 110 (1977) 341.
[11] L.W. Schmid and J.E. Hearst, J. Mol. Biol. 44 (1969) 143.
[12] S.B. Leighton and K. Rubenstein, J. Mol.Biol. 46 (1969) 313.
[13] S.B. Dubin, G.B. Benedek, F.C. Bancroft and D. Freifelder, J. Mol. Biol. 54 (1970) 547.
[14] D. Lang, J. Mol. Biol. 54 (1970) 557.
[15] M. Weissman, H. Schindler and G. Feher, Proc. Nat. Acad. Sci., Wash. 73 (1976) 2776.
[16] M.H. Adams, Bacteriophages (Interscience Publishers, Inc., New York, 1959) p. 446.
[17] H.R. Massie and B.H. Zimm, Proc. Nat. Acad. Sci., Wasl 54 (1965) 1641.
[18] H.R. Massie and B.H. Zimm, Biopolymers 7 (1969) 475
[19] I. Rubenstein, C.A. Thomas Jr. and A.D. Hershey, Proc Nat. Acad. Sci., Wash. 47 (1961) 1113.
[20] L.C. Klotz and B.H. Zimm, Macromolecules 5 (1972) 471.
[21] B.H. Zimm and D.M. Crothers, Proc. Nat. Acad. Sci., Wash. 48 (1962) 905.
[22] H. Sober, Handbook biochemistry and molecular biolog (2nd ed., The Chemical Rubber Company, Cleveland, Ohio, 1970).
[23] B.D. Bowen and B.H. Zimm, Manuscript in preparation.
[24] P.E. Rouse Jr., J. Chem. Phys. 21 (1953) 1272.
[25] B.H. Zimm, J. Chem. Phys. 24 (1956) 269.
[26] N.W. Tschoegl, J. Chem. Phys. 40 (1964) 473.
[27] N.W. Tschoegl, J. Chem. Phys. 39 (1963) 149.
[28] O.B. Ptitsyn and Y.E. Eisner, Zh. Fiz. Khim. 32 (1958) 2464.
[29] V.A. Bloomfield, and B.H. Zimm, J. Chem. Phys. 44 (1966) 315.
[30] V.A. Bloomfield, D.M. Crothers and I. Tinoco Jr., Physical chemistry of nucleic acids (Harper and Row, New York, 1974).
[31] K. Dill and R.H. Shafer, Biophys. Chem. 4 (1976) 51.
[32] K. Osaki, Macromolecules 5 (1972) 141.
[33] N.W. Tschoegl, private communication, Manuscript in process of being published.
[34] F.W. Wang, J. Polym. Sci., Polym. Phys. Ed. 13 (1975) 1215.
[35] F.W. Wang, J. Polym. Sci., Polym. Phys. Ed. 12 (1974) 1619.
[36] J.E. Hearst and W.H. Stockmayer, J. Chem. Phys. 37 (1962) 1425.
[37] M.T. Record Jr., C.P. Woodbury and R.B. Inman, Biopolymers 14 (1975) 393.
[38] J.B. Hays, M.E. Magar and B.H. Zimm, Biopolymers 8 (1969) 531.
[39] D.M. Crothers and B.H. Zimm, J. Mol. Biol. 12 (1965) 525.
[40] B.C. Bowen, Ph.D. dissertation, University of California San Diego, (1977).
[41] V.N. Schumaker and C. Bennett, J. Mol. Biol. 5 (1962) 384.
[42] P.D. Ross and R.L. Scruggs, Biopolymers 6 (1968) 1005
[43] L.A. Holmes, K. Ninomya and J.D. Ferry, J. Phys. Chen 70 (1966) 2714.
[44] G. Felsenfeld and S.Z. Hirschman, J. Mol. Biol. 13 (1965) 407.
[45] H. Margenau and G.M. Murphy, Mathematics of Physics and Chemistry (1st Ed., Van Nostrand, New York, 1943) p. 500.
[46] D. Freifelder, J. Mol. Biol. 54 (1970) 567.